Programmable Quantum Processors based on Spin Qubits with Mechanically-Mediated Interactions and Transport

F. Fung,[1] E. Rosenfeld,[1,*] J. D. Schaefer,[1] A. Kabcenell,[1] J. Gieseler,[1]
T. X. Zhou,[1,2,3,†] T. Madhavan,[2] N. Aslam,[1,4] A. Yacoby,[1] and M. D. Lukin[1,‡]

[1] *Department of Physics, Harvard University, Cambridge, Massachusetts, 02138, USA*
[2] *Harvard John A. Paulson School of Engineering and Applied Sciences, Harvard University, Cambridge, Massachusetts, 02138, USA*
[3] *Massachusetts Institute of Technology, Cambridge, Massachusetts, 02139, USA*
[4] *Institute of Condensed Matter Physics, Technische Universität Braunschweig, Braunschweig, Germany*

Solid state spin qubits are promising candidates for quantum information processing, but controlled interactions and entanglement in large, multi-qubit systems are currently difficult to achieve. We describe a method for programmable control of multi-qubit spin systems, in which individual nitrogen-vacancy (NV) centers in diamond nanopillars are coupled to magnetically functionalized silicon nitride mechanical resonators in a scanning probe configuration. Qubits can be entangled via interactions with nanomechanical resonators while programmable connectivity is realized via mechanical transport of qubits in nanopillars. To demonstrate the feasibility of this approach, we characterize both the mechanical properties and the magnetic field gradients around the micromagnet placed on the nanobeam resonator. Furthermore, we show coherent manipulation and mechanical transport of a proximal spin qubit by utilizing nuclear spin memory, and use the NV center to detect the time-varying magnetic field from the oscillating micromagnet, extracting a spin-mechanical coupling of 7.7(9) Hz. With realistic improvements the high-cooperativity regime can be reached, offering a new avenue towards scalable quantum information processing with spin qubits.

Introduction. Isolated spin defects in the solid state, such as nitrogen vacancy (NV) centers in diamond, have long been considered as promising candidates for quantum information processing, owing to their extended coherence times even at elevated temperatures [1–5]. While small spin registers have been realized using coupled electronic and nuclear spins [6–8], such demonstrations rely on magnetic dipole-dipole interactions, which limit the distance between spins to tens of nanometers. The short-range nature of these interactions and imprecision of defect fabrication at these length scales make it challenging to control systems containing large arrays of spin qubits.

Several approaches are currently being explored to address this challenge, including long-range entanglement based on photonic [9, 10] and mechanical systems [11, 12]. In particular, nanomechanical resonators have been proposed as a mesoscopic interface between distant and otherwise isolated spin qubits. Such a hybrid quantum system can be realized by combining electronic spins with magnetically functionalized mechanical resonators [13–24]. Mechanical resonators can be engineered to have very high quality factors with flexible, compact geometric realizations, and feature low crosstalk relative to their electromagnetic counterparts [25]. Using mechanical modes as a quantum transducer, distant spin qubits can be entangled deterministically, even when the mechanical mode is in a thermal, highly excited state [11, 26, 27]. Furthermore, spin qubits can be used to cool the mechanical resonator to its ground state [28, 29] and subsequently prepare non-Gaussian states of motion [30]. Despite these intriguing proposals, realizing the necessary strong coupling between mechanical systems and individual spin qubits is a challenging task, requiring deterministic positioning of spin qubits in close proximity to magnetized mechanical resonators. Moreover, even though transducers extend the spin-spin interaction range, the system connectivity remains local, limiting its programmability and scalability.

In this Letter, we introduce a novel platform for realizing programmable interactions between distant spin qubits. The key idea of our architecture is illustrated in Fig. 1(a). In our approach, individual NV centers in diamond nanopillars are coupled to silicon nitride nanobeam mechanical resonators in a scanning probe geometry. A micromagnet attached to the nanobeam provides the magnetic field gradient for the spin-mechanical coupling. Ultra-high quality factors $Q > 10^9$ have been demonstrated in silicon nitride mechanical resonators through a combination of techniques such as soft-clamping, dissipation dilution, and strain engineering [31–35]. At the same time, the nanoscale footprint of the diamond nanopillar enables small separations between the NV center and the micromagnet [36, 37], providing access to high magnetic field gradients required for large spin-mechanical coupling. Remarkably, spin qubits confined in nanopillars can be moved mechanically in and out of the near-field of the magnetized resonators. Moreover, they can be transported across relatively long (10-100 μm) distances, enabling non-local connectivity between distant qubits [38–43]. Further improvements in coherence time can be obtained by making use of a nuclear spin quantum mem-

* Currently at AWS Center for Quantum Computing, Pasadena, California, 91106, USA
† Currently at Northrop Grumman Mission Systems, Linthicum, Maryland, 21090, USA
‡ lukin@physics.harvard.edu

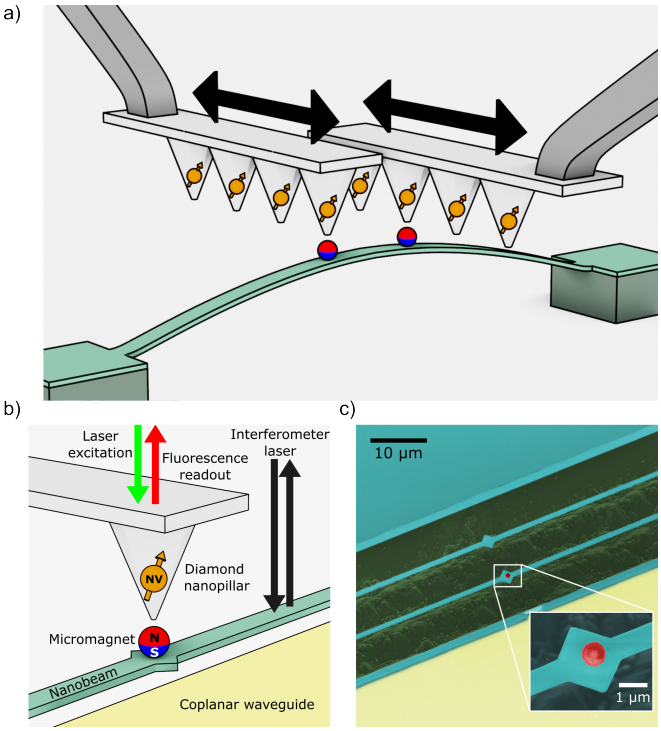

FIG. 1. (a) Conceptual diagram for programmable interactions within arrays of nanopillars containing spin qubits. Spin qubits (orange) can be micro-manipulated (black arrows) to interact with a common mechanical mode of a magnetically-functionalized resonator (turquoise), enabling mechanically-mediated spin-spin interactions. (b) Our current experimental realization: a diamond nanopillar containing a single NV center at its tip is positioned above an NdFeB spherical micromagnet at the center of a doubly clamped silicon nitride nanobeam. The nanobeam is fabricated on the same chip as a coplanar waveguide which facilitates coherent microwave control of the NV center's electronic spin. The chip is mounted on a 3-axis nanopositioner stack, while the diamond nanopillar is kept fixed. (c) False-color scanning electron microscope image of the nanobeam (turquoise lines, two shown) with a micromagnet (red sphere) placed on a pad at the antinode of motion. The gold area at the bottom of the image is the coplanar waveguide for microwave delivery. Inset: zoom-in image of the micromagnet.

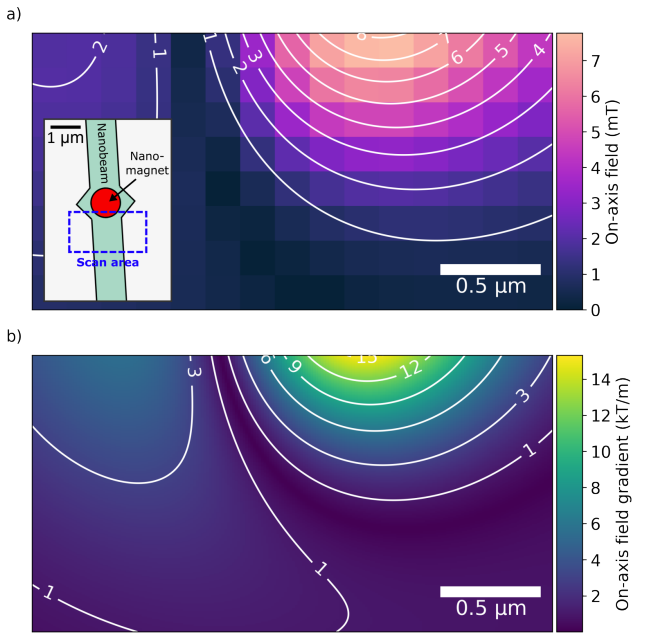

FIG. 2. Magnetic field imaging of a micromagnet. (a) Magnetic field in an area around the magnet, with a vertical NV-magnet separation of about 1 μm. For each position of the diamond nanopillar, we measure the electron spin resonance (ESR) frequencies, from which we extract the magnetic field along the NV center's axis [45]. The field from the spherical micromagnet is well-approximated by a dipole model, with the fit (contours) deviating from the measured fields by no more than 3 G at any point. The orientations of the NV center and magnet are consistent with the fabrication process of the nanopillar and magnetization direction respectively. These measurements were performed in air at room temperature, without any external driving of the mechanical resonator. Inset: Diagram showing the scanning area around the micromagnet on the nanobeam. (b) Reconstructed magnetic field gradients based on fit to dipole model. The maximum gradient is $\sim 1.5 \times 10^4$ T/m.

ory. Since the latter is less sensitive to magnetic fields, such storage can be used for long-distant qubit transport even in the presence of proximal magnetic gradients, enabling reconfigurable quantum processing architecture similar to that demonstrated recently for neutral atom array qubits [38].

To demonstrate the feasibility of this approach, we first perform scanning magnetometry with the nanopillar to characterize the magnetic field and field gradients around a micromagnet. Subsequently, as a proof-of-principle demonstration of coherent transport, we store coherent information inside the NV center's intrinsic ^{15}N nuclear spin, and show that the spin coherence is not affected by movement over 1.7(2) μm near the micromagnet. Finally, by measuring the mechanical motion interferometrically and using the NV center to detect the time-varying magnetic field from the oscillating micromagnet, we extract the single-phonon spin-mechanical coupling strength of 7.7(9) Hz. With realistic improvements to our quality factors and further reduction in the magnet-NV center distance, the coherent coupling regime is within reach.

Experimental setup and static magnetic field characterization. Our experimental platform consists of a scanning probe setup, where a diamond nanopillar containing a single NV center is positioned near a micromagnet placed at the center of the nanobeam (Fig. 1(b, c)). In addition to improving the optical collection efficiency, the nanopillar has a small surface area at its apex, allowing for nanoscale magnet-NV center distances [36, 37, 44].

The presence of a magnetic field perpendicular to the NV center quantization axis limits NV spin readout contrast, photoluminesence intensity, and coherence time

$T_{2,e}$ in a natural-abundance ^{13}C diamond [46]. In order to align the magnetic field and characterize the field distribution, we scan the micromagnet with respect to the diamond nanopillar with a 3-axis stack of piezoelectric nanopositioners. At each position, we optically measure the electron spin resonance (ESR) and calculate the magnetic field along the NV center quantization axis [45]; an example map of the magnetic field around a micromagnet is shown in Fig. 2(a). With our current smallest micromagnet-NV distance of $\sim 1.0\,\mu$m, we estimate gradients exceeding 1.5×10^4 T/m, corresponding to an expected single-phonon spin-mechanical coupling strength of $\lambda/2\pi \sim 5$ Hz (Fig. 2(b)).

Preservation of spin coherence while moving in a magnetic field gradient. Next, to investigate whether the spin coherence can be maintained during qubit transport, we perform a proof-of-principle experiment in which we move the micromagnet 1.7(2) µm away from the diamond nanopillar and then back to its original position. Pulsed ESR measurements at different times during the movement sequence (Fig. 3 (a)) reveal a significant change in the magnetic field environment, as evidenced by a shift of 9.8(1) MHz in the ESR frequency [45].

We demonstrate the preservation of spin coherence while moving in a magnetic field gradient, using the pulse sequence in Fig. 3(b) synchronized with the movement sequence in Fig. 3(a). Since the total movement time of 1.7 ms is significantly longer than the electronic spin coherence time of 0.95(4) ms [45], we use the NV center's intrinsic ^{15}N nuclear spin as a quantum memory [47, 48] to enable the mechanical qubit transport.

Specifically, in our demonstration the electron and ^{15}N nuclear spin are first initialized in a two-qubit register $|-1\rangle_e \otimes |\downarrow\rangle_n$ [45], followed by a $\pi/2$-pulse which puts the ^{15}N nuclear spin in a superposition $|-1\rangle_e \otimes (|\downarrow\rangle + |\uparrow\rangle)_n$. Subsequently, we apply a C_nNOT_e gate which fully entangles the electron-nucleus pair $-|0\rangle_e |\downarrow\rangle_n + |-1\rangle_e |\uparrow\rangle_n$.

During the subsequent free evolution time τ, the entangled electron-nucleus pair accumulates a phase $\phi(\tau)$. For the particular NV center in our measurements, hyperfine interactions with a nearby ^{13}C nuclear spin lead to phase accumulation at a rate of ~ 0.9 MHz. A second C_nNOT_e gate then disentangles the electron-nuclear pair and the phase information $\phi(\tau)$ is now entirely stored in the ^{15}N nuclear spin $|-1\rangle_e \otimes \left(-|\downarrow\rangle + e^{i\phi(\tau)}|\uparrow\rangle\right)_n$.

As shown in Fig. 3(a), the field at the nanopillar changes significantly during the movement sequence, leading to an additional phase accumulation on the ^{15}N. We eliminate this additional phase by applying a π-pulse on the ^{15}N near the middle of the movement sequence [45]. Finally, a $\pi/2$-pulse at the end of the movement sequence converts the stored phase information $\phi(\tau)$ into the probability of finding the ^{15}N in either $|\downarrow\rangle_n$ or $|\uparrow\rangle_n$, which can be measured with a boost in signal-to-noise ratio (SNR) using repetitive readout [49].

By fixing $\tau = 900\,\text{ns} < T^*_{2,e}$ and varying the rotation axis angle of the final $\pi/2$-pulse, we can quantify the spin coherence preservation. The results, shown in

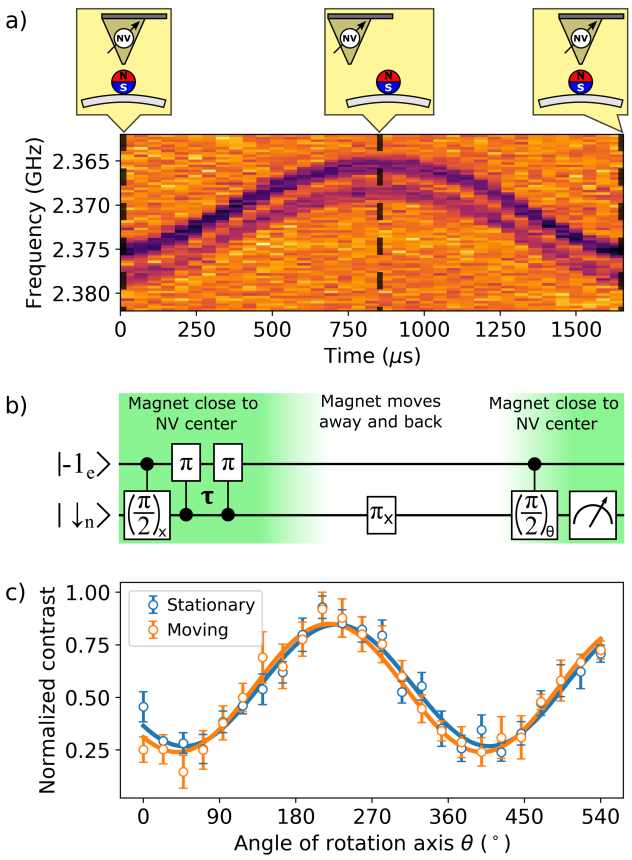

FIG. 3. Preservation of spin coherence while moving in a magnetic field gradient. (a) The nanobeam along with the micromagnet is moved 1.7(2) µm from the NV center and then back to its original position over 1.7 ms. Pulsed ESR measurements at different times during the movement sequence show the changing field from the moving micromagnet. The 3 MHz hyperfine splitting from the NV center's intrinsic ^{15}N nuclear spin is clearly visible; an additional hyperfine splitting from a nearby ^{13}C nuclear spin is not shown here due to the microwave pulse duration used [45]. (b) Pulse sequence used to demonstrate storage and retrieval of coherent information, synchronized with the movement sequence shown in (a). (c) Fixing the phase accumulation time $\tau = 900$ ns, we measure the coherence of the nuclear spin at the end of the movement sequence by varying the rotation axis angle θ of the final $\pi/2$-pulse, for both cases where the micromagnet is moved (orange) and kept stationary (blue).

3(c) demonstrate that the normalized contrasts for cases where the micromagnet is moved (orange) and kept stationary (blue) are 0.61(3) and 0.57(3) respectively, indicating that the nuclear spin coherence is unaffected by the significant change in magnetic field.

Mechanical motion and single-phonon coupling strength. Finally, we characterize the spin-mechanical coupling by exciting the nanobeam and characterizing its mechanical motion via independent measurements with both an interferometer and the nearby NV center. To take advantage of higher quality factors at

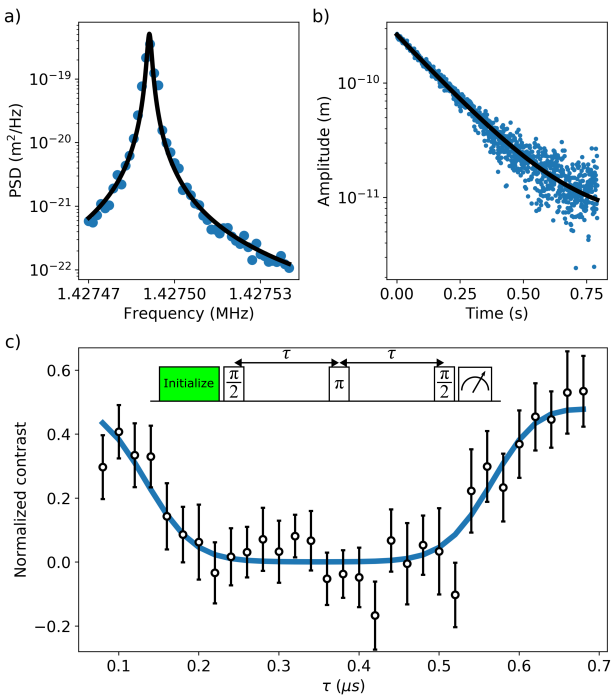

FIG. 4. Sensing the mechanical motion of the nanobeam. (a) Power spectral density (PSD) of the mechanical mode, measured using an interferometer. From the Lorentzian fit (black line) we extract a resonance frequency of $\sim 1.4\,\mathrm{MHz}$ and a linewidth of $\kappa/2\pi = 1.5(2)\,\mathrm{Hz}$. (b) After switching off an external drive from a piezoelectric chip, we measure the amplitude decay of the mechanical motion and obtain $Q = 8.25(6) \times 10^5$. **(c)** Sensing of the mechanical motion with the NV center. We perform a Hahn echo pulse sequence on the NV center with and without the mechanical drive, and plot their ratio (black circles) such that we can neglect the NV center's decoherence in our model for the fit ($\chi(\tau)$, blue line). We fit the signal $S(\tau, \lambda, \Delta_x)/e^{-\chi(\tau)}$ (see eq. (1)), using fixed values of Δ_x and ω_r from interferometer measurements, to find $\lambda/2\pi = 7.7(9)\,\mathrm{Hz}$. The zero-point motion z_p is inferred from the material densities and dimensions of the mechanical resonator.

low temperatures, we use the scanning probe setup in a helium cryostat. The interferometric measurements, shown in Fig. 4(a,b), reveal a quality factor of $8.25(6) \times 10^5$ (Fig. 4(b)), demonstrating that the quality factor remains high despite magnetic functionalization [45]. The mechanical frequency $\omega_r \sim 1.4\,\mathrm{MHz}$ (Fig. 4(a)) corresponds to a period of $0.7\,\mu\mathrm{s}$. As a result, the mechanical resonator can undergo multiple oscillations during the spin coherence time $T_{2,e}$, which is around several microseconds. The readily accessible high mechanical frequency of the nanobeam compares favorably to other spin-mechanical platforms, such as those featuring cantilevers, nanowires, and magnetic levitation [13, 17, 23].

A displacement of the mechanical mode by the zero-point fluctuation z_p shifts the NV center spin resonance by $\lambda/2\pi$ via the Zeeman effect, resulting in the single-phonon coupling strength $\lambda = \gamma_e z_p \nabla_z$, where γ_e is the NV center electronic spin gyromagnetic ratio, and ∇_z is the magnetic field gradient along the NV center quantization axis. To quantify the spin-mechanical coupling strength, we excite the nanobeam with an external broadband drive and detect the field from the oscillating micromagnet with the nearby NV center. We use a Hahn echo pulse sequence, which results in frequency-dependent detection of the magnetic spin environment [45]. Sweeping the time τ between the π pulses and assuming a Gaussian distribution of the mechanical state, the spin contrast can be approximated as

$$S(\tau, \lambda, \Delta_x) = \alpha e^{-8\Delta_x^2\lambda^2 \sin^4(\omega_r\tau/2)/\omega_r^2 z_p^2} e^{-\chi(\tau)} \qquad (1)$$

where Δ_x is the root-mean-squared amplitude of motion, α is the spin readout contrast, and $\chi(\tau)$ describes the coherence decay from other noise sources in the diamond, such as the bath of ^{13}C nuclear spins [46] [45].

To determine λ, we first independently quantify Δ_x by integrating the interferometer signal of the mechanical response from the wideband drive, and assign ω_r to the center frequency. For the data corresponding to figure 4(a), we find that $\Delta_x = 1.86(1)$ nm. We then fit the Hahn echo data, normalized to a baseline Hahn echo measurement to compensate for intrinsic NV decoherence $e^{-\chi(\tau)}$ (Fig. 4(c), black dots). For the fit (blue line), ω_r and Δ_x are fixed, leaving λ as a free parameter. We find that $\lambda/2\pi = 7.7(9)\,\mathrm{Hz}$ (Fig. 4(b), corresponding to a gradient of $2.4(1) \times 10^4\,\mathrm{T/m}$, similar to the gradients from the static field imaging of the same magnet (Fig. 2(b)).

Discussion and Outlook. Our experiments demonstrate the feasibility of the proposed architecture for programmable mechanically-mediated interactions between distant spins. Specifically, we showed that the NV center's intrinsic nuclear spin memory is not degraded by movement inside a field gradient, if the proper decoupling pulse sequences are applied. The demonstrated movement distance of $1.7(2)\,\mu\mathrm{m}$ in Fig. 3(a-c) significantly exceeds the range of magnetic dipole-dipole interactions between spins, and is limited by the moving speed of $1\,\mathrm{mm/s}$ and nuclear spin coherence time $T_{2,n} \sim 5\,\mathrm{ms}$ [45]. The speed can be increased by using a nanopositioner with a higher bandwidth and minimizing residual vibrations caused by the scanning motion. By decoupling the nuclear spin from its local environment or cooling to cryogenic temperatures, $T_{2,n}$ can be extended to $> 1\,\mathrm{s}$ [2, 50], which would extend the possible distance to $> 1\,\mathrm{mm}$ even with the current speed.

At the same time, achieving quantum coherent spin-mechanical coupling [14, 26, 27, 29, 51, 52] requires increasing the coupling strength while minimizing noise. Specifically, the onset of coherent quantum phenomena is generally marked by the spin-mechanical cooperativity $C \equiv \frac{\lambda^2}{\Gamma\kappa n_{th}} \gtrsim 1$, which compares the coherent coupling rate λ to the dissipation rates $\Gamma, \kappa n_{th}$ of the spin and mechanical mode respectively. While the cooperativity of our present experiment exceeds previous spin-

mechanical platforms involving NV centers [45], it remains far below the coherent coupling regime. However, significant improvements can be made. Drift of the NV-magnet distance causes significant variations of the ESR frequency at high magnetic field gradients, limiting our current gradient to 2.4×10^4 T/m at a distance of 1.0 µm. With improvements to the setup stability and the use of atomic-force microscopy (AFM) feedback [36, 53], positioning the NV center at a reduced distance of 50 nm from the surface of a 1 µm-diameter micromagnet should yield gradients $\sim 1.4 \times 10^6$ T/m, or a spin-mechanical coupling of $\lambda/2\pi \sim 800$ Hz. The doubly clamped nanobeam can be replaced with recent designs that utilize strain engineering and soft-clamping, which have demonstrated $Q \sim 10^9$ at MHz frequencies [31, 32, 34, 35, 54]. Even higher quality factors have been demonstrated or predicted, by replacing silicon nitride with crystalline materials such as silicon and diamond [55, 56]. For a coupling strength of $\lambda/2\pi = 800$ Hz, an NV center electronic spin coherence time $T_{2,e}$ of 10 ms [7, 57], and a quality factor of 10^9 at 4 K, the coherent coupling regime is possible with $C \sim 75$. Under such conditions, mechanics-mediated entanglement of electronic spins with fidelity exceeding 95 % should be feasible according to the proposal in [27]. Although we expect $T_{2,e}$ to improve with larger NV implantation depth, further investigation into diamond fabrication and surface termination might be required to increase $T_{2,e}$ to the 10 ms regime for NV centers in diamond nanopillars [58, 59].

Compared to previous work involving on-chip, circuit-based hybrid quantum systems [11, 30], a spin-mechanical architecture featuring dynamical qubit transport has the advantage of being able to generate programmable, non-local interactions, similar to reconfigurable platforms based on neutral atoms and trapped ions. The long coherence time of the nuclear spin allows multiple distant spins to be dynamically transported to interact with the same mechanical bus. While Fig. 1 only shows one mechanical resonator for clarity, the architecture can also be parallelized, with multiple mechanical resonators simultaneously mediating interactions within large arrays of spins. We also note that, unlike most other hybrid quantum systems [23, 30], both the mechanical and spin components of our platform are highly coherent even at room temperature. With a nanomagnet diameter of 0.3 µm, an NV-magnet separation of 20 nm, spin coherence time of $T_{2,e} = 2$ ms [60], and $Q = 1 \times 10^9$, reaching the coherent-coupling regime at room temperature appears feasible. The above considerations indicate that with realistic improvements, our platform can enable programmable interactions between distant spins, opening up a new avenue towards scalable quantum information processing with solid-state spin qubits. Finally, the present approach can be extended to realize other hybrid systems by coupling spin qubits to quantum systems such as superconducting qubits and optical photons [25, 61, 62].

Acknowledgements We thank M. Markham and Element Six for providing diamond samples, R. Walsworth and M. Turner for annealing diamonds, K. Van Kirk, D. Bluvstein, A. Mulski, and E. Polzik for helpful discussions, B. Machielse for assistance with fabrication, R. Riedinger for comments on the manuscript, S. Y. F. Zhou and A. Cui for assistance with sample magnetization, and A. S. Zibrov and J. MacArthur for technical assistance. This work was supported by NSF, Center for Ultracold Atoms, and DOE Quantum Systems Accelerator Center (contract no. 7568717). E. R. acknowledges support from the NSF Graduate Research Fellowship Program. A. K. acknowledges support from the DOD through the NDSEG Fellowship Program. J. G. acknowledges support by the European Union (SEQOO, H2020-MSCA-IF-2014, No. 655369). Diamond and resonator sample fabrication were performed at the Center for Nanoscale Systems (CNS), a member of the National Nanotechnology Coordinated Infrastructure, which is supported by the NSF under award no. ECCS -1541959. CNS is part of Harvard University. T. X. Z is an affiliate to Center for Quantum Network (CQN) established by NSF to facilitate collaboration within CQN to advance quantum research. T.M. acknowledges support from the NSF Graduate Research Fellowship Program (grant 2140743). N.A. acknowledges support from the Alexander von Humboldt Foundation and by the Federal Ministry of Education and Research (BMBF, project “13N16297”).

[1] G. Balasubramanian, P. Neumann, D. Twitchen, M. Markham, R. Kolesov, N. Mizuochi, J. Isoya, J. Achard, J. Beck, J. Tissler, V. Jacques, P. R. Hemmer, F. Jelezko, and J. Wrachtrup, Ultralong spin coherence time in isotopically engineered diamond, Nat. Mat. **8**, 383 (2009).

[2] P. C. Maurer, G. Kucsko, C. Latta, L. Jiang, N. Y. Yao, S. D. Bennett, F. Pastawski, D. Hunger, N. Chisholm, M. Markham, D. J. Twitchen, J. I. Cirac, and M. D. Lukin, Room-temperature quantum bit memory exceeding one second, Science **336**, 1283 (2012).

[3] M. Widmann, S.-Y. Lee, T. Rendler, N. T. Son, H. Fedder, S. Paik, L.-P. Yang, N. Zhao, S. Yang, I. Booker, *et al.*, Coherent control of single spins in silicon carbide at room temperature, Nat. Mat. **14**, 164 (2015).

[4] C. P. Anderson, E. O. Glen, C. Zeledon, A. Bourassa, Y. Jin, Y. Zhu, C. Vorwerk, A. L. Crook, H. Abe, J. Ul-Hassan, *et al.*, Five-second coherence of a single spin with single-shot readout in silicon carbide, Sci. Adv. **8**, eabm5912 (2022).

[5] P.-J. Stas, Y. Q. Huan, B. Machielse, E. N. Knall, A. Suleymanzade, B. Pingault, M. Sutula, S. W. Ding, C. M.

Knaut, D. R. Assumpcao, *et al.*, Robust multi-qubit quantum network node with integrated error detection, Science **378**, 557 (2022).
[6] M. V. G. Dutt, L. Childress, L. Jiang, E. Togan, J. Maze, F. Jelezko, A. Zibrov, P. Hemmer, and M. Lukin, Quantum register based on individual electronic and nuclear spin qubits in diamond, Science **316**, 1312 (2007).
[7] M. H. Abobeih, J. Cramer, M. A. Bakker, N. Kalb, M. Markham, D. J. Twitchen, and T. H. Taminiau, One-second coherence for a single electron spin coupled to a multi-qubit nuclear-spin environment, Nat. Commun. **9**, 2552 (2018).
[8] C. E. Bradley, J. Randall, M. H. Abobeih, R. C. Berrevoets, M. J. Degen, M. A. Bakker, M. Markham, D. J. Twitchen, and T. H. Taminiau, A ten-qubit solid-state spin register with quantum memory up to one minute, Phys. Rev. X **9**, 031045 (2019).
[9] M. K. Bhaskar, R. Riedinger, B. Machielse, D. S. Levonian, C. T. Nguyen, E. N. Knall, H. Park, D. Englund, M. Lončar, D. D. Sukachev, *et al.*, Experimental demonstration of memory-enhanced quantum communication, Nature **580**, 60 (2020).
[10] S. L. N. Hermans, M. Pompili, H. K. C. Beukers, S. Baier, J. Borregaard, and R. Hanson, Qubit teleportation between non-neighbouring nodes in a quantum network, Nature **605**, 663 (2022).
[11] P. Rabl, S. J. Kolkowitz, F. H. L. Koppens, J. G. E. Harris, P. Zoller, and M. D. Lukin, A quantum spin transducer based on nanoelectromechanical resonator arrays, Nat. Phys. **6**, 602 (2010).
[12] M. C. Kuzyk and H. Wang, Scaling phononic quantum networks of solid-state spins with closed mechanical subsystems, Phys. Rev. X **8**, 041027 (2018).
[13] O. Arcizet, V. Jacques, A. Siria, P. Poncharal, P. Vincent, and S. Seidelin, A single nitrogen-vacancy defect coupled to a nanomechanical oscillator, Nat. Phys. **7**, 879 (2011).
[14] S. D. Bennett, S. Kolkowitz, Q. P. Unterreithmeier, P. Rabl, A. C. B. Jayich, J. G. E. Harris, and M. D. Lukin, Measuring mechanical motion with a single spin, New J. Phys. **14**, 125004 (2012).
[15] S. Kolkowitz, A. C. B. Jayich, Q. P. Unterreithmeier, S. D. Bennett, P. Rabl, J. G. E. Harris, and M. D. Lukin, Coherent sensing of a mechanical resonator with a single-spin qubit, Science **335**, 1603 (2012).
[16] J. M. Nichol, E. R. Hemesath, L. J. Lauhon, and R. Budakian, Nanomechanical detection of nuclear magnetic resonance using a silicon nanowire oscillator, Phys. Rev. B **85**, 054414 (2012).
[17] D. Rugar, R. Budakian, H. J. Mamin, and B. W. Chui, Single spin detection by magnetic resonance force microscopy, Nature **430**, 329 (2004).
[18] J. Teissier, A. Barfuss, P. Appel, E. Neu, and P. Maletinsky, Strain coupling of a nitrogen-vacancy center spin to a diamond mechanical oscillator, Phys. Rev. Lett. **113**, 020503 (2014).
[19] B. Pigeau, S. Rohr, L. Mercier de Lépinay, A. Gloppe, V. Jacques, and O. Arcizet, Observation of a phononic mollow triplet in a multimode hybrid spin-nanomechanical system, Nat. Commun. **6**, 8603 (2015).
[20] K. W. Lee, D. Lee, P. Ovartchaiyapong, J. Minguzzi, J. R. Maze, and A. C. B. Jayich, Strain coupling of a mechanical resonator to a single quantum emitter in diamond, Phys. Rev. Appl. **6**, 034005 (2016).
[21] S. Meesala, Y.-I. Sohn, H. A. Atikian, S. Kim, M. J. Burek, J. T. Choy, and M. Lončar, Enhanced strain coupling of nitrogen-vacancy spins to nanoscale diamond cantilevers, Phys. Rev. Appl. **5**, 034010 (2016).
[22] T. Oeckinghaus, S. A. Momenzadeh, P. Scheiger, T. Shalomayeva, A. Finkler, D. Dasari, R. Stöhr, and J. Wrachtrup, Spin–phonon interfaces in coupled nanomechanical cantilevers, Nano Lett. **20**, 463 (2020).
[23] J. Gieseler, A. Kabcenell, E. Rosenfeld, J. D. Schaefer, A. Safira, M. J. A. Schuetz, C. Gonzalez-Ballestero, C. C. Rusconi, O. Romero-Isart, and M. D. Lukin, Single-spin magnetomechanics with levitated micromagnets, Phys. Rev. Lett. **124**, 163604 (2020).
[24] S. Maity, L. Shao, S. Bogdanović, S. Meesala, Y.-I. Sohn, N. Sinclair, B. Pingault, M. Chalupnik, C. Chia, L. Zheng, K. Lai, and M. Lončar, Coherent acoustic control of a single silicon vacancy spin in diamond, Nat. Commun. **11**, 193 (2020).
[25] Y. Chu and S. Gröblacher, A perspective on hybrid quantum opto-and electromechanical systems, Appl. Phys. Lett. **117**, 150503 (2020).
[26] M. J. A. Schuetz, G. Giedke, L. M. K. Vandersypen, and J. I. Cirac, High-fidelity hot gates for generic spin-resonator systems, Phys. Rev. A **95**, 052335 (2017).
[27] E. Rosenfeld, R. Riedinger, J. Gieseler, M. Schuetz, and M. D. Lukin, Efficient entanglement of spin qubits mediated by a hot mechanical oscillator, Phys. Rev. Lett. **126**, 250505 (2021).
[28] P. Rabl, P. Cappellaro, M. V. G. Dutt, L. Jiang, J. R. Maze, and M. D. Lukin, Strong magnetic coupling between an electronic spin qubit and a mechanical resonator, Phys. Rev. B **79**, 041302 (2009).
[29] P. Rabl, Cooling of mechanical motion with a two-level system: The high-temperature regime, Phys. Rev. B **82**, 165320 (2010).
[30] A. D. O'Connell, M. Hofheinz, M. Ansmann, R. C. Bialczak, M. Lenander, E. Lucero, M. Neeley, D. Sank, H. Wang, M. Weides, J. Wenner, J. M. Martinis, and A. N. Cleland, Quantum ground state and single-phonon control of a mechanical resonator, Nature **464**, 697 (2010).
[31] Y. Tsaturyan, A. Barg, E. S. Polzik, and A. Schliesser, Ultracoherent nanomechanical resonators via soft clamping and dissipation dilution, Nat. Nanotechnol. **12**, 776 (2017).
[32] A. H. Ghadimi, S. A. Fedorov, N. J. Engelsen, M. J. Bereyhi, R. Schilling, D. J. Wilson, and T. J. Kippenberg, Elastic strain engineering for ultralow mechanical dissipation, Science **360**, 764 (2018).
[33] M. J. Bereyhi, A. Beccari, S. A. Fedorov, A. H. Ghadimi, R. Schilling, D. J. Wilson, N. J. Engelsen, and T. J. Kippenberg, Clamp-tapering increases the quality factor of stressed nanobeams, Nano Lett. **19**, 2329 (2019).
[34] J. Guo and S. Gröblacher, Integrated optical-readout of a high-q mechanical out-of-plane mode, Light Sci. Appl. **11**, 282 (2022).
[35] M. J. Bereyhi, A. Beccari, R. Groth, S. A. Fedorov, A. Arabmoheghi, T. J. Kippenberg, and N. J. Engelsen, Hierarchical tensile structures with ultralow mechanical dissipation, Nat. Commun. **13**, 3097 (2022).
[36] T. X. Zhou, R. J. Stöhr, and A. Yacoby, Scanning diamond nv center probes compatible with conventional afm technology, Appl. Phys. Lett. **111**, 163106 (2017).

[37] P. Maletinsky, S. Hong, M. S. Grinolds, B. Hausmann, M. D. Lukin, R. L. Walsworth, M. Loncar, and A. Yacoby, A robust scanning diamond sensor for nanoscale imaging with single nitrogen-vacancy centres, Nat. Nanotechnol. **7**, 320 (2012).

[38] D. Bluvstein, H. Levine, G. Semeghini, T. T. Wang, S. Ebadi, M. Kalinowski, A. Keesling, N. Maskara, H. Pichler, M. Greiner, V. Vuletić, and M. D. Lukin, A quantum processor based on coherent transport of entangled atom arrays, Nature **604**, 451–456 (2022).

[39] T. Đorđević, P. Samutpraphoot, P. L. Ocola, H. Bernien, B. Grinkemeyer, I. Dimitrova, V. Vuletić, and M. D. Lukin, Entanglement transport and a nanophotonic interface for atoms in optical tweezers, Science **373**, 1511 (2021).

[40] O. Mandel, M. Greiner, A. Widera, T. Rom, T. W. Hänsch, and I. Bloch, Coherent transport of neutral atoms in spin-dependent optical lattice potentials, Phys. Rev. Lett. **91**, 010407 (2003).

[41] J. M. Pino, J. M. Dreiling, C. Figgatt, J. P. Gaebler, S. A. Moses, M. S. Allman, C. H. Baldwin, M. Foss-Feig, D. Hayes, K. Mayer, *et al.*, Demonstration of the trapped-ion quantum ccd computer architecture, Nature **592**, 209 (2021).

[42] C. Monroe, R. Raussendorf, A. Ruthven, K. R. Brown, P. Maunz, L.-M. Duan, and J. Kim, Large-scale modular quantum-computer architecture with atomic memory and photonic interconnects, Phys. Rev. A **89**, 022317 (2014).

[43] J. I. Cirac and P. Zoller, A scalable quantum computer with ions in an array of microtraps, Nature **404**, 579 (2000).

[44] L. Xie, T. X. Zhou, R. J. Stöhr, and A. Yacoby, Crystallographic orientation dependent reactive ion etching in single crystal diamond, Adv. Mat. **30**, 1705501 (2018).

[45] See Supplemental Material.

[46] P. L. Stanwix, L. M. Pham, J. R. Maze, D. Le Sage, T. K. Yeung, P. Cappellaro, P. R. Hemmer, A. Yacoby, M. D. Lukin, and R. L. Walsworth, Coherence of nitrogen-vacancy electronic spin ensembles in diamond, Phys. Rev. B **82**, 201201 (2010).

[47] M. Pfender, N. Aslam, H. Sumiya, S. Onoda, P. Neumann, J. Isoya, C. A. Meriles, and J. Wrachtrup, Nonvolatile nuclear spin memory enables sensor-unlimited nanoscale spectroscopy of small spin clusters, Nat. Commun. **8**, 834 (2017).

[48] S. Zaiser, T. Rendler, I. Jakobi, T. Wolf, S.-Y. Lee, S. Wagner, V. Bergholm, T. Schulte-Herbrüggen, P. Neumann, and J. Wrachtrup, Enhancing quantum sensing sensitivity by a quantum memory, Nat. Commun. **7**, 12279 (2016).

[49] L. Jiang, J. S. Hodges, J. R. Maze, P. Maurer, J. M. Taylor, D. G. Cory, P. R. Hemmer, R. L. Walsworth, A. Yacoby, A. S. Zibrov, and M. D. Lukin, Repetitive readout of a single electronic spin via quantum logic with nuclear spin ancillae, Science **326**, 267 (2009).

[50] M. Pfender, N. Aslam, P. Simon, D. Antonov, G. Thiering, S. Burk, F. Fávaro de Oliveira, A. Denisenko, H. Fedder, J. Meijer, and et al., Protecting a diamond quantum memory by charge state control, Nano Lett. **17**, 5931 (2017).

[51] A. Vinante, M. Bahrami, A. Bassi, O. Usenko, G. Wijts, and T. H. Oosterkamp, Upper bounds on spontaneous wave-function collapse models using millikelvin-cooled nanocantilevers, Phys. Rev. Lett. **116**, 090402 (2016).

[52] J. Van Wezel and T. H. Oosterkamp, A nanoscale experiment measuring gravity's role in breaking the unitarity of quantum dynamics, Proc. R. Soc. A. **468**, 35 (2012).

[53] A. Ariyaratne, D. Bluvstein, B. A. Myers, and A. C. B. Jayich, Nanoscale electrical conductivity imaging using a nitrogen-vacancy center in diamond, Nat. Commun. **9**, 2406 (2018).

[54] M. J. Bereyhi, A. Arabmoheghi, A. Beccari, S. A. Fedorov, G. Huang, T. J. Kippenberg, and N. J. Engelsen, Perimeter modes of nanomechanical resonators exhibit quality factors exceeding 10 9 at room temperature, Phys. Rev. X **12**, 021036 (2022).

[55] A. Beccari, D. A. Visani, S. A. Fedorov, M. J. Bereyhi, V. Boureau, N. J. Engelsen, and T. J. Kippenberg, Strained crystalline nanomechanical resonators with quality factors above 10 billion, Nat. Phys. **18**, 436 (2022).

[56] L. Sementilli, E. Romero, and W. P. Bowen, Nanomechanical dissipation and strain engineering, Adv. Funct. Mater. **32**, 2105247 (2022).

[57] N. Bar-Gill, L. M. Pham, A. Jarmola, D. Budker, and R. L. Walsworth, Solid-state electronic spin coherence time approaching one second, Nat. Commun. **4**, 1743 (2013).

[58] L. Luan, M. S. Grinolds, S. Hong, P. Maletinsky, R. L. Walsworth, and A. Yacoby, Decoherence imaging of spin ensembles using a scanning single-electron spin in diamond, Sci. Rep. **5**, 8119 (2015).

[59] S. Sangtawesin, B. L. Dwyer, S. Srinivasan, J. J. Allred, L. V. H. Rodgers, K. De Greve, A. Stacey, N. Dontschuk, K. M. O'Donnell, D. Hu, D. A. Evans, C. Jaye, D. A. Fischer, M. L. Markham, D. J. Twitchen, H. Park, M. D. Lukin, and N. P. de Leon, Origins of diamond surface noise probed by correlating single-spin measurements with surface spectroscopy, Phys. Rev. X **9**, 031052 (2019).

[60] E. D. Herbschleb, H. Kato, Y. Maruyama, T. Danjo, T. Makino, S. Yamasaki, I. Ohki, K. Hayashi, H. Morishita, M. Fujiwara, *et al.*, Ultra-long coherence times amongst room-temperature solid-state spins, Nat. Commun. **10**, 3766 (2019).

[61] A. A. Clerk, K. W. Lehnert, P. Bertet, J. R. Petta, and Y. Nakamura, Hybrid quantum systems with circuit quantum electrodynamics, Nat. Phys. **16**, 257 (2020).

[62] S. Barzanjeh, A. Xuereb, S. Gröblacher, M. Paternostro, C. A. Regal, and E. M. Weig, Optomechanics for quantum technologies, Nat. Phys. **18**, 15 (2022).